Pakistan Journal of Statistics and Operation Research

The New Topp-Leone-Heavy-Tailed Type II Exponentiated Half Logistic-G Family of Distributions: Properties, Actuarial Measures, with Applications to Censored Data

Wibert Nkomo[1*], Broderick Oluyede[2] and Fastel Chipepa[3]

*Corresponding author

1. Department of Mathematics and Statistical Sciences, Botswana International University of Science and Technology, Botswana & Manicaland State University of Applied Sciences, Zimbabwe, willynkomo@gmail.com
2. Department of Mathematics and Statistical Sciences, Botswana International University of Science and Technology, Botswana, oluyedeo@biust.ac.bw
3. Department of Mathematics and Statistical Sciences, Botswana International University of Science and Technology, Botswana, chipepaf@biust.ac.bw

Abstract

The Topp-Leone heavy-tailed type II exponentiated half logistic-G (TL-HT-TIIEHL-G) is the newly proposed family of distributions (FoDs) introduced in this research. The study thoroughly investigates the statistical properties of this FoDs, as well as its relevance in actuarial risk assessment. The estimation of the unknown model parameters is done using the method of maximum likelihood estimation, and the consistency of these estimates is assessed through the implementation of Monte Carlo simulations. Additionally, numerical simulations are conducted to analyze the risk measures associated with the TL-HT-TIIEHL-G FoDs. The Topp-Leone heavy-tailed type II exponentiated half logistic-Weibull (TL-HT-TIIEHL-W) distribution, a particular case of the TL-HT-TIIEHL-G FoDs is compared with other contending distributions including heavy-tailed distributions to evaluate its performance. The model's capacity, adaptability, and practicality are convincingly showcased through its application to real data.

Key Words: Topp-Leone-G; Heavy-tailed-G; Exponentiated half logistic distribution; Estimation; Censoring; Moments; Risk measures.

Mathematical Subject Classification: 60E05, 62E15.

1. Introduction

In many fields of applied research, the final part of a study frequently consists of a thorough examination of the acquired data. Lifespan data are well-known for conveying a large amount of information that must be captured in order to identify some significant occurrences. Most prominent classical distributions often fail to match and anticipate data from a range of practical disciplines, including finance, medical sciences and environmental sciences, engineering, and economics. As a result, certain generalized FoDs are believed to constitute a step forward in establishing and broadening the standard classical distributions. The newly developed FoDs have undergone extensive research across various disciplines, demonstrating their remarkable versatility and broad applicability. Due to their inherent adaptability, these generalized families have garnered substantial utilization for the purpose of data modeling across a wide array of domains.

In recent times, several authors have made significant contributions to the development of an extensive range of extended families of distributions. These extended families of distributions include, the type II general inverse exponential by Jamal et al. (2020), Topp-Leone odd exponential half logistic-G by Chipepa and Oluyede (2021), type II Quasi-Lambert-G by Hamedani et al. (2020), Topp-Leone Harris-G by Oluyede et al. (2023), the type I heavy-tailed by Zhao et al. (2020), type II exponentiated half logistic by Al-Mofleh et al. (2020), new generalized logarithmic–X by Shah et al. (2023), generalised odd Fréchet by Marganpoor et al. (2020), Topp-Leone Gompertz-G by Oluyede et al. (2022), and the gamma Topp-Leone type II exponetiated half logistic-G by Oluyede and Moakofi (2023) among others.

In their study, Al-Shomrani et al. (2016) pioneered the Topp-Leone-G (TL-G) FoDs. This family has its cumulative distribution function (cdf) and corresponding probability density function (pdf), defined as follows:

$$F(x;b,\Omega)=\left[1-\bar{G}^{2}(x;\Omega)\right]^{b} \tag{1}$$

and

$$f(x;b,\Omega)=2bg(x;\Omega)\bar{G}(x;\Omega)\left[1-\bar{G}^{2}(x;\Omega)\right]^{b-1}, \tag{2}$$

respectively, where $b,x>0$ and Ω is a parameter vector from the baseline distribution $G(.)$. Note that $1-G(x;\Omega)=\bar{G}(x;\Omega)$. Zhao et al. (2020) proposed the type I heavy-tailed (HT-G) FoDs with the cdf

$$F(x;\alpha,\Gamma)=1-\left(\frac{\bar{G}(x;\Gamma)}{1-(1-\alpha)G(x;\Gamma)}\right)^{\alpha} \tag{3}$$

and pdf

$$f(x;\alpha,\Gamma) = \frac{\alpha^{2}g(x;\Gamma)\left[\bar{G}(x;\Gamma)\right]^{\alpha-1}}{\left[1-(1-\alpha)G(x;\Gamma)\right]^{\alpha+1}}, \tag{4}$$

respectively, for $\alpha,x>0$, where Γ is a parameter vector from the baseline distribution $G(.)$. Replacing the baseline cdf in Equation (1) with the HT-G distribution yields the Topp-Leone-heavy-tailed-G (TL-HT-G) FoDs with cdf

$$F(x;b,\alpha,\Gamma)=\left[1-\left(\frac{\bar{G}(x;\Gamma)}{1-(1-\alpha)G(x;\Gamma)}\right)^{2\alpha}\right]^{b}, \tag{5}$$

and pdf

$$f(x;b,\alpha,\Gamma) = 2b\alpha^{2}g(x;\Gamma)\left[\bar{G}(x;\Gamma)\right]^{2\alpha-1}\frac{\left[1-\left(\frac{\bar{G}(x;\Gamma)}{1-(1-\alpha)G(x;\Gamma)}\right)^{2\alpha}\right]^{b-1}}{\left[1-(1-\alpha)G(x;\Gamma)\right]^{2\alpha+1}}, \tag{6}$$

respectively, for $b,\alpha,x>0$ and Γ is a parameter vector from the baseline distribution $G(.)$

In this study, we introduce a novel FoDs named Topp-Leone-heavy-tailed type II exponentiated half-logistic-G (TL-HT-TIIEHL-G). The TL-HT-TIIEHL-G FoDs have demonstrated exceptional data fitting versatility, as evidenced by their ability to accommodate diverse density and hazard rate geometries in the special models. Several motivations led to the development of this paradigm, including:

(i) utilizing the TL-HT-G and the TIIEHL-G FoDs to increase the capabilities of the current families of distributions;

(ii) expanding the range of potential parental density functions and hazard rate functions (hrf);

(iii) developing heavy-tailed distributions to model real data from a variety of domains;

(iv) exploring how the TL-HT-TIIEHL-G FoDs can be effectively used to model censored data, enabling more reliable analysis and prediction in situations where complete information is lacking;

(v) evaluating the ability of the TL-HT-TIIEHL-G FoDs to accurately represent risk measures thereby facilitating informed decision-making and risk management strategies.

The following describes how the paper is structured. We develop the new FoDs, its sub-families, statistical properties and special cases for specified baseline distributions in Section 2. In Section 3, we conduct the estimation of parameters. We discuss risk measures in Section 4. Section 5 of the study is dedicated to presenting the results of the simulations conducted. In Section 6, various data examples are provided, and the concluding observations of the research are presented in Section 7.

2. The New FoDs and its Properties

The authors Al-Mofleh et al. (2020) proposed the type II exponentiated half-logistic-G (TIIEHL-G) FoDs with cdf

$$F(x;\omega,\delta,\varpi) \quad = \quad 1-\left[\frac{1-[G(x;\varpi)]^{\omega}}{1+[G(x;\varpi)]^{\omega}}\right]^{\delta} \tag{7}$$

and pdf

$$f(x;\omega,\delta,\varpi) \quad = \quad 2\delta\omega g(x;\varpi)\frac{(1-[G(x;\varpi)]^{\omega})^{\delta-1}[G(x;\varpi)]^{\omega-1}}{(1+[G(x;\varpi)]^{\omega})^{\delta+1}}, \tag{8}$$

where x, ω, and δ are all positive. Note that the function $g(x;\varpi)$ represents the pdf of the baseline distribution, while $G(x;\varpi)$ represents the cdf of the baseline distribution, with the parameter vector ϖ. We shall set $\omega=1$ to circumvent over-parametrization. We shall also set $D_G(x;\delta,\varpi)=\left[\frac{1-G(x;\varpi)}{1+G(x;\varpi)}\right]^{\delta}$ in this paper.

Replacing the baseline cdf in Equation (5) with the TIIEHL-G cdf yields a new FoDs called Topp-Leone heavy-tailed type II exponentiated half-logistic-G (TL-HT-TIIEHL-G) FoDs. The cdf, survival function and pdf are given by

$$F(x;\alpha,\delta,b,\varpi) \quad = \quad \left[1-\left(\frac{D_G(x;\delta,\varpi)}{1-(1-\alpha)\left[1-D_G(x;\delta,\varpi)\right]}\right)^{2\alpha}\right]^{b}, \tag{9}$$

$$S(x;\alpha,\delta,b,\varpi) \quad = \quad 1-\left[1-\left(\frac{D_G(x;\delta,\varpi)}{1-(1-\alpha)\left[1-D_G(x;\delta,\varpi)\right]}\right)^{2\alpha}\right]^{b} \tag{10}$$

and

$$\begin{aligned} f(x;\alpha,\delta,b,\varpi) \quad &= \quad 4b\delta\alpha^{2}g(x;\varpi)\frac{[\bar{G}(x;\varpi)]^{\delta-1}}{[1+G(x;\varpi)]^{\delta+1}}\left[1-\left(\frac{D_G(x;\delta,\varpi)}{1-(1-\alpha)\left[1-D_G(x;\delta,\varpi)\right]}\right)^{2\alpha}\right]^{b-1} \\ &\times \quad \left(\frac{[D_G(x;\delta,\varpi)]^{2\alpha-1}}{\left[1-(1-\alpha)\left[1-D_G(x;\delta,\varpi)\right]\right]^{2\alpha+1}}\right), \end{aligned} \tag{11}$$

respectively, where $x,\alpha,\delta,b>0$. The hazard rate function (hrf) of the TL-HT-TIIEHL-G FoDs is

$$h(x;\alpha,\delta,b,\varpi) = 4b\delta\alpha^2 g(x;\varpi)\left[1-\left(\frac{D_G(x;\delta,\varpi)}{1-(1-\alpha)\left[1-D_G(x;\delta,\varpi)\right]}\right)^{2\alpha}\right]^{b-1}\left(\frac{\left[D_G(x;\delta,\varpi)\right]^{2\alpha-1}}{\left[1-(1-\alpha)\left[1-D_G(x;\delta,\varpi)\right]\right]^{2\alpha+1}}\right)$$
$$\times \frac{[\bar{G}(x;\varpi)]^{\delta-1}}{[1+G(x;\varpi)]^{\delta+1}}\left(1-\left[1-\left(\frac{D_G(x;\delta,\varpi)}{1-(1-\alpha)\left[1-D_G(x;\delta,\varpi)\right]}\right)^{2\alpha}\right]^{b}\right)^{-1}. \quad (12)$$

2.1. Density Function Series Expansion

The pdf of the new TL-HT-TIIEHL-G FoDs can be written as

$$f(x;\alpha,\delta,b,\varpi) = \sum_{r=0}^{\infty}\Phi_{r+1}g_{r+1}(x;\varpi), \quad (13)$$

where $g_{r+1}(x;\varpi)=(r+1)g(x;\varpi)G^r(x;\varpi)$ represents the exponentiated-G (Expo-G) distribution with power parameter $(r+1)$ and

$$\Phi_{r+1} = 4b\delta\alpha^2\sum_{l,m,n,p,q=0}^{\infty}(-1)^{l+m+n+q+r}(1-\alpha)^m\binom{b-1}{l}\binom{1+2\alpha(l+1)}{m}\binom{m}{n}\binom{p+\delta[n+2\alpha(l+1)+2]}{p}\binom{p}{q}$$
$$\times \binom{q+\delta[n+2\alpha(l+1)+2]-1}{r}\left(\frac{1}{r+1}\right), \quad (14)$$

is the linear component. Consequently, the TL-HT-TIIEHL-G FoDs is can be expressed as an infinite linear combination of Expo-G densities, allowing for the direct derivation of various statistical properties. See **web appendix** for details.

2.2. Quantile Function

The quantile function of the TL-HT-TIIEHL-G FoDs is

$$Q_X(u)=G^{-1}\left(\frac{1+\left(\frac{(1-u^{\frac{1}{b}})^{\frac{1}{2\alpha}}-(1-\alpha)(1-u^{\frac{1}{b}})^{\frac{1}{2\alpha}}}{1-(1-\alpha)(1-u^{\frac{1}{b}})^{\frac{1}{2\alpha}}}\right)^{\delta}}{1-\left(\frac{(1-u^{\frac{1}{b}})^{\frac{1}{2\alpha}}-(1-\alpha)(1-u^{\frac{1}{b}})^{\frac{1}{2\alpha}}}{1-(1-\alpha)(1-u^{\frac{1}{b}})^{\frac{1}{2\alpha}}}\right)^{\delta}}\right),$$

where $u\in[0,1]$ for $\alpha,\delta,b>0$. Consequently, the quantile values can be obtained by utilizing R software to solve the non-linear equation based on a given baseline cdf G(.). See **web appendix** for derivations.

2.3. Moments and Incomplete Moments

If Y_{r+1} is an Expo-G distributed random variable with power parameter $(r+1)$, then the p^{th} moment of the new FoDs is

$$E(X^p) = \sum_{r=0}^{\infty}\Phi_{r+1}E(Y_{r+1}^p),$$

where Φ_{r+1} is specified in Equation (14) and $E(Y_{r+1}^p)$ is the p^{th} moment of Y_{r+1}. The p^{th} incomplete moment is

$$I_X(t)=\int_0^t x^p f(x)dx=\sum_{r=0}^{\infty}\Phi_{r+1}I_{r+1}(t;p,\varpi),$$

where $I_{r+1}(t;p,\varpi)=\int_0^t x^p g_{r+1}(x;\varpi)dx$ represents the p^{th} incomplete moment of Y_{r+1}. The moment generating function (MGF) of X is

$$M_X(t) = \sum_{r=0}^{\infty}\Phi_{r+1}E(e^{tY_{r+1}}),$$

where $E(e^{tY_{r+1}})$ is the MGF of Y_{r+1} and Φ_{r+1} is specified in Equation (14).

Incomplete moments are crucial in the construction of Bonferroni and Lorenz curves for the TL-HT-TIIEHL-G FoDs, while complete moments are valuable in the computation of coefficients of variation, skewness, kurtosis, and other related characteristics.

2.4. Order Statistics

The pdf of the h^{th} order statistics derived from the TL-HT-TIIEHL-G FoDs is

$$f_{h:n}(x) = \frac{1}{B(h,n-h+1)}\sum_{z=0}^{\infty}\sum_{j=0}^{n-h}\binom{n-h}{j}\Phi^{*}_{z+1}g_{z+1}(x;\varpi), \tag{15}$$

where $B(.,.)$ is the beta function, $g_{z+1}(x;\varpi)=g(x;\varpi)(z+1)G^{z}(x;\varpi)$ represents the Expo-G distribution with power parameter $(z+1)$ and

$$\begin{aligned}\Phi^{*}_{z+1} &= 4b\delta\alpha^{2}\sum_{q,r,s,t,u,v,w=0}^{\infty}(-1)^{s+t+u+v+w+z}(1-\alpha)^{r}\binom{b+(j+h)-1}{q}\binom{2\alpha+(q+1)+r}{r}\binom{r+2\alpha-1}{s}\\ &\times \binom{s+\delta-1}{t}\binom{s+\delta-1}{u}\binom{u}{v}\binom{v-(s+\delta-1)}{w}\binom{w}{z}\left(\frac{1}{z+1}\right).\end{aligned}$$

In light of this, the pdf of the h^{th} order statistics from the TL-HT-TIIEHL-G FoDs is expressible as an infinite linear combination of the Expo-G densities. Refer to the **web appendix** section for detailed derivations.

2.5. Probability Weighted Moments

The probability weighted moments (PWMs) for the TL-HT-TIIEHL-G FoDs can be written as

$$M_{(q,r,v)} = \sum_{i=0}^{\infty}\alpha^{*}_{i+1}\int_{-\infty}^{\infty}x^{q}g_{i+1}(x;\varpi)dx, \tag{16}$$

where $g_{i+1}(x;\varpi)=(i+1)g(x;\varpi)G^{i}(x;\varpi)$ is the Expo-G distribution with power parameter $(i+1)$ and

$$\begin{aligned}\alpha^{*}_{i+1} &= 4b\delta\alpha^{2}\sum_{a,c,d,e,f,g,h=0}^{\infty}(-1)^{a+c+e+f+g+h+i}(1-\alpha)^{d}\binom{v}{a}\binom{a+b(r-1)-1}{c}\binom{2\alpha(c+1)+d}{d}\binom{d}{e}\\ &\times \binom{e+\delta+f}{f}\binom{f}{g}\binom{g+\delta-1}{h}\binom{g+h}{i}\left(\frac{1}{i+1}\right).\end{aligned}$$

Consequently, we can obtain the $(q,r,v)^{th}$ PMWs of the TL-HT-TIIEHL-G FoDs from the moments of the Expo-G FoDs. See **web appendix** for derivations.

2.6. Stochastic Ordering

Stochastic (st) ordering possesses applications within the realm of probability and statistics. They serve practical purposes in probability theory by enabling the deduction of probability inequalities and facilitating the comparison of lifetime distributions based on specific characteristics.

Consider two random variables, U and V, which have distribution functions denoted as $F_U(t)$ and $F_V(t)$, respectively and $\bar{F}_U(t) = 1 - F_U(t)$ denotes the survival function. Note that U is stochastically smaller than V if $\bar{F}_U(t) \leq \bar{F}_V(t)\ \forall t$ or $F_U(t) \geq F_V(t)\ \forall t$. This is denoted by $U <_{st} V$. The hazard rate order (hr) and likelihood ratio (lr) order possess greater strength compared to the stochastic and is given by $U <_{hr} V$ if $h_U(t) \geqslant h_V(t)\ \forall t$, and $U <_{lr} V$ if $\frac{h_U(t)}{h_V(t)}$ is decreasing in t (see Shaked and Shanthikumar (2007) for further details). We know that $U <_{lr} V \Rightarrow U <_{hr} V \Rightarrow U <_{st} V$.

Theorem: Let X_1 and X_2 be independent random variables with $X_1 \sim TL-HT-TIIEHL-G(\alpha,\delta,b_1,\varpi)$ and $X_2 \sim TL-HT-TIIEHL-G(\alpha,\delta,b_2,\varpi)$, respectively. If $b_2 > b_1$, then the random variables X_1 and X_2 are stochastically ordered.

Proof: Note that,

$$f_1(x;\alpha,\delta,b_1,\varpi) = \frac{4b_1\delta\alpha^2 g(x;\varpi)[1-G(x;\varpi)]^{\delta-1}}{[1+G(x;\varpi)]^{\delta+1}}\left[1-\left(\frac{D_G(x;\delta,\varpi)}{1-(1-\alpha)[1-D_G(x;\delta,\varpi)]}\right)^{2\alpha}\right]^{b_1-1} \times \left(\frac{[D_G(x;\delta,\varpi)]^{2\alpha-1}}{[1-(1-\alpha)(1-D_G(x;\delta,\varpi))]^{2\alpha+1}}\right), \quad (17)$$

and

$$f_2(x;\alpha,\delta,b_2,\varpi) = \frac{4b_2\delta\alpha^2 g(x;\varpi)[1-G(x;\varpi)]^{\delta-1}}{[1+G(x;\varpi)]^{\delta+1}}\left[1-\left(\frac{D_G(x;\delta,\varpi)}{1-(1-\alpha)[1-D_G(x;\delta,\varpi)]}\right)^{2\alpha}\right]^{b_2-1} \times \left(\frac{[D_G(x;\delta,\varpi)]^{2\alpha-1}}{[1-(1-\alpha)(1-D_G(x;\delta,\varpi))]^{2\alpha+1}}\right), \quad (18)$$

so that

$$\frac{f_1(x)}{f_2(x)} = \frac{f_1(x;\alpha,\delta,b_1,\varpi)}{f_2(x;\alpha,\delta,b_2,\varpi)} = \frac{b_1}{b_2}\left[1-\left(\frac{D_G(x;\delta,\varpi)}{1-(1-\alpha)[1-D_G(x;\delta,\varpi)]}\right)^{2\alpha}\right]^{b_1-b_2}. \quad (19)$$

Differentiating Equation (19) with respect to x, yields

$$\frac{\partial}{\partial x}\left(\frac{f_1(x)}{f_2(x)}\right) = \frac{b_1}{b_2}(b_1-b_2)\left[1-\left(\frac{D_G(x;\delta,\varpi)}{1-(1-\alpha)[1-D_G(x;\delta,\varpi)]}\right)^{2\alpha}\right]^{b_1-b_2-1} \times \frac{\partial}{\partial x}\left[\left(\frac{D_G(x;\delta,\varpi)}{1-(1-\alpha)[1-D_G(x;\delta,\varpi)]}\right)^{2\alpha}\right].$$

Now, if $b_1 < b_2$, then $\frac{\partial}{\partial x}\left(\frac{f_1(x)}{f_2(x)}\right) < 0$. Therefore, likelihood ratio exists between X_1 and X_2. As a result, the random variables X_1 and X_2 are stochastically ordered.

2.7. Entropy

Entropy measures the degree of uncertainty present in a probability distribution. The two widely used measures of entropy are the Rényi entropy introduced by Rényi (1960), and the Shannon entropy proposed by Shannon (1950).

The Rényi entropy for the TL-HT-TIIEHL-G FoDs can be expressed as

$$I_R(\omega)=\frac{\log\left[\sum_{m=0}^{\infty}\varepsilon_m e^{[(1-\omega)I_{REG}]}\right]}{1-\omega},\omega\neq 1,\omega>0, \tag{20}$$

where

$$\begin{aligned}\varepsilon_m &= \sum_{i,j,k,l=0}^{\infty}(-1)^{i+k+l+m}(4b\delta)^{\omega}\alpha^{2\omega}(1-\alpha)^j\binom{\omega(b-1)}{i}\binom{2\alpha(i+\omega)+\omega)+j-1}{j}\binom{2\alpha(i+\omega)-\omega\delta+k}{k}\\ &\times \binom{k}{l}\binom{l+2\alpha(i+\omega)+\omega(\delta+1)}{m}\left(\frac{l}{\omega}+1\right),\end{aligned}$$

and $I_{REG}=\left[\int_0^{\infty}\left(\frac{l}{\omega}+1\right)[g(x;\varpi)G^{\frac{m}{\omega}}(x;\varphi)]dx\right]^{\omega}$ is the Rényi entropy of the Expo-G distribution with parameter $(\frac{l}{\omega}+1)$. As a result, Rényi entropy of the TL-HT-TIIEHL-G FoDs stem directly from Rényi entropy of the Expo-G distribution. See **web appendix** for derivations.

2.8. TL-HT-TIIEHL-G Sub-Families

Table [1] presents various sub-families associated with the TL-HT-TIIEHL-G FoDs, accompanied by their corresponding nomenclature. The sub-families are also new families of distributions.

Table 1: Sub-families of TL-HT-TIIEHL-G FoDs

α	δ	b	Resultant Distribution	Distribution Nomenclature
1	-	-	$F(x;\delta,b,\varpi)=\left[1-\left(\frac{1-G(x;\varpi)}{1+G(x;\varpi)}\right)^{2\delta}\right]^b$	Topp-Leone type II exponentiated half logistic-G FoDs
-	1	-	$F(x;\alpha,b,\varpi)=\left[1-\left(\frac{\left[\frac{1-G(x;\varpi)}{1+G(x;\varpi)}\right]}{1-(1-\alpha)\left[1-\left[\frac{1-G(x;\varpi)}{1+G(x;\varpi)}\right]\right]}\right)^{2\alpha}\right]^b$	Topp-Leone-heavy-tail type II half logistic-G FoDs
-	-	1	$F(x;\alpha,\delta,\varpi)=1-\left(\frac{\left[\frac{1-G(x;\varpi)}{1+G(x;\varpi)}\right]^{\delta}}{1-(1-\alpha)\left[1-\left[\frac{1-G(x;\varpi)}{1+G(x;\varpi)}\right]^{\delta}\right]}\right)^{2\alpha}$	Heavy-tailed type II exponentiated half logistic-G FoDs
1	1	-	$F(x;b,\varpi)=\left[1-\left(\frac{1-G(x;\varpi)}{1+G(x;\varpi)}\right)^{2}\right]^b$	Topp-Leone type II half logistic-G FoDs
1	-	1	$F(x;\delta,\varpi)=1-\left(\frac{1-G(x;\varpi)}{1+G(x;\varpi)}\right)^{2\delta}$	A new FoDs
-	1	1	$F(x;\alpha,\varpi)=1-\left(\frac{\left(\frac{1-G(x;\varpi)}{1+G(x;\varpi)}\right)}{1-(1-\alpha)\left[1-\left(\frac{1-G(x;\varpi)}{1+G(x;\varpi)}\right)\right]}\right)^{2\alpha}$	Heavy-tailed type II half logistic-G FoDs
1	1	1	$F(x;\varpi)=1-\left(\frac{1-G(x;\varpi)}{1+G(x;\varpi)}\right)^{2}$	A new FoDs

2.9. Particular Cases

This subsection presents some special cases of TL-HT-TIIEHL-G FoDs by specifying the baseline cdf and pdf in Equations (9) and (11). The log-logistic, uniform, and Weibull distributions are considered as baseline cdf in this section.

2.9.1. Topp-Leone-Heavy-Tailed-Type II Exponentiated Half Logistic-Log-Logistic (TL-HT-TIIEHL-LLoG) Distribution

Considering the log-logistic distribution with the cdf and pdf given by $G(x;\beta)=1-\frac{1}{1+x^{\beta}}$ and $g(x;\beta)=\frac{\beta x^{\beta-1}}{(1+x^{\beta})^{2}}$ as baseline distribution, for $x,\beta>0$, we have the TL-HT-TIIEHL-LLoG distribution with cdf

$$F(x;\alpha,\delta,b,\beta) = \left[1-\left(\frac{[A_1(x;\beta)]^{\delta}}{1-(1-\alpha)\left(1-[A_1(x;\beta)]^{\delta}\right)}\right)^{2\alpha}\right]^{b}$$

and pdf

$$\begin{aligned} f(x;\alpha,\delta,b,\beta) &= 4b\delta\alpha^{2}\left[1-\left(\frac{[A_1(x;\beta)]^{\delta}}{1-(1-\alpha)\left(1-[A_1(x;\beta)]^{\delta}\right)}\right)^{2\alpha}\right]^{b-1}\frac{\beta x^{\beta-1}(1+x^{\beta})^{-(\delta+1)}}{[2-(1+x^{\beta})^{-1}]^{\delta+1}} \\ &\times \left(\frac{[A_1(x;\beta)]^{\delta(2\alpha-1)}}{\left[1-(1-\alpha)\left(1-[A_1(x;\beta)]^{\delta}\right)\right]^{2\alpha+1}}\right), \end{aligned}$$

where $A_1(x;\beta)=\frac{(1+x^{\beta})^{-1}}{2-(1+x^{\beta})^{-1}}$ for $\alpha,\delta,b,\beta,x>0$. The hrf is

$$\begin{aligned} h(x;\alpha,\delta,b,\beta) &= 4b\delta\alpha^{2}\left[1-\left(\frac{[A_1(x;\beta)]^{\delta}}{1-(1-\alpha)\left(1-[A_1(x;\beta)]^{\delta}\right)}\right)^{2\alpha}\right]^{b-1}\frac{\beta x^{\beta-1}(1+x^{\beta})^{-(\delta+1)}}{[2-(1+x^{\beta})^{-1}]^{\delta+1}} \\ &\times \left(\frac{[A_1(x;\beta)]^{\delta(2\alpha-1)}}{\left[1-(1-\alpha)\left(1-[A_1(x;\beta)]^{\delta}\right)\right]^{2\alpha+1}}\right)\left(1-\left[1-\left(\frac{[A_1(x;\beta)]^{\delta}}{1-(1-\alpha)\left(1-[A_1(x;\beta)]^{\delta}\right)}\right)^{2\alpha}\right]^{b}\right)^{-1}. \end{aligned}$$

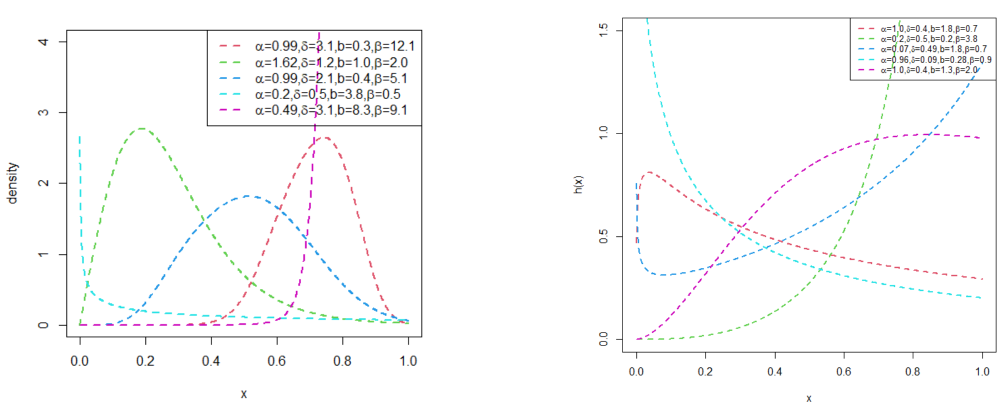

Figure 1: Density and hrf plots for the TL-HT-TIIEHL-LLoG distribution

Figure [1] presents density and hrf plots of the TL-HT-TIIEHL-LLoG distribution. The density plot demonstrates the distribution's ability to accommodate positively skewed, negatively skewed, near symmetric, J and reversed-J shaped data. Additionally, the hrf plot can effectively handle both monotonic and non-monotonic shapes. It is worth noting that non-monotonic shapes are commonly encountered in real-life scenarios.

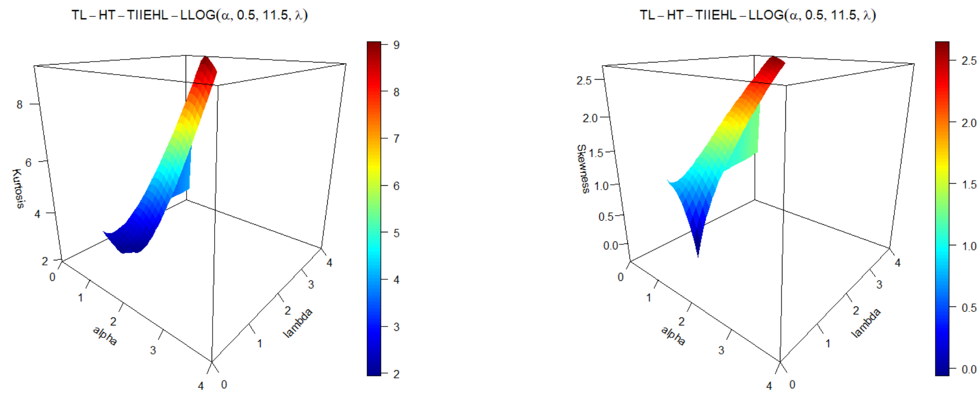

Figure 2: Some 3D plots of the TL-HT-TIIEHL-LLOG distribution's skewness and kurtosis

After controlling for δ and b, Figure [2] demonstrates that both kurtosis and skewness increase with increasing α and λ for the TL-HT-TIIEHL-LLOG distribution.

2.9.2. Topp-Leone-Heavy-Tailed-Type II Exponentiated Half Logistic Uniform (TL-HT-TIIEHL-U) Distribution

The uniform distribution has cdf $G(x;\theta)=\frac{x}{\theta}$ and $g(x;\theta)=\frac{1}{\theta}$ for $0<x<\theta$. The TL-HT-TIIEHL-U distribution is derived by using the uniform distribution as the baseline. The TL-HT-TIIEHL-U cdf is

$$F(x;\alpha,\delta,b,\theta) = \left[1-\left(\frac{(\theta-x)^{\delta}}{(\theta+x)^{\delta}\left[1-(1-\alpha)\left(1-[A_2(x;\theta)]^{\delta}\right)\right]}\right)^{2\alpha}\right]^{b}$$

and pdf is

$$\begin{aligned} f(x;\alpha,\delta,b,\theta) &= \frac{4b\delta\alpha^2}{\theta}\left[1-\left(\frac{(\theta-x)^{\delta}}{(\theta+x)^{\delta}\left[1-(1-\alpha)\left(1-[A_2(x;\theta)]^{\delta}\right)\right]}\right)^{2\alpha}\right]^{b-1} \\ &\times \frac{(\frac{\theta-x}{\theta})^{\delta-1}}{(\frac{\theta+x}{\theta})^{\delta+1}}\left(\frac{[\theta-x]^{\delta(2\alpha-1)}}{(\theta+x)^{\delta(2\alpha-1)}\left[1-(1-\alpha)\left(1-[A_2(x;\theta)]^{\delta}\right)\right]^{2\alpha+1}}\right)\end{aligned}$$

for $\alpha,\delta,b,\theta,x>0$, where $A_2(x;\theta)=\frac{\theta-x}{\theta+x}$. The hrf is

$$\begin{aligned} h(x;\alpha,\delta,b,\theta) &= \frac{4b\delta\alpha^2}{\theta}\left[1-\left(\frac{(\theta-x)^{\delta}}{(\theta+x)^{\delta}\left[1-(1-\alpha)\left(1-[A_2(x;\theta)]^{\delta}\right)\right]}\right)^{2\alpha}\right]^{b-1} \\ &\times \frac{(\frac{\theta-x}{\theta})^{\delta-1}}{(\frac{\theta+x}{\theta})^{\delta+1}}\left(\frac{[\theta-x]^{\delta(2\alpha-1)}}{(\theta+x)^{\delta(2\alpha-1)}\left[1-(1-\alpha)\left(1-[A_2(x;\theta)]^{\delta}\right)\right]^{2\alpha+1}}\right) \\ &\times \left(1-\left[\left[1-\left(\frac{(\theta-x)^{\delta}}{(\theta+x)^{\delta}\left[1-(1-\alpha)\left(1-[A_2(x;\theta)]^{\delta}\right)\right]}\right)^{2\alpha}\right]^{b}\right]\right)^{-1}.\end{aligned}$$

 DOI: https://doi.org/10.18187/pjsor.v21i2.4640

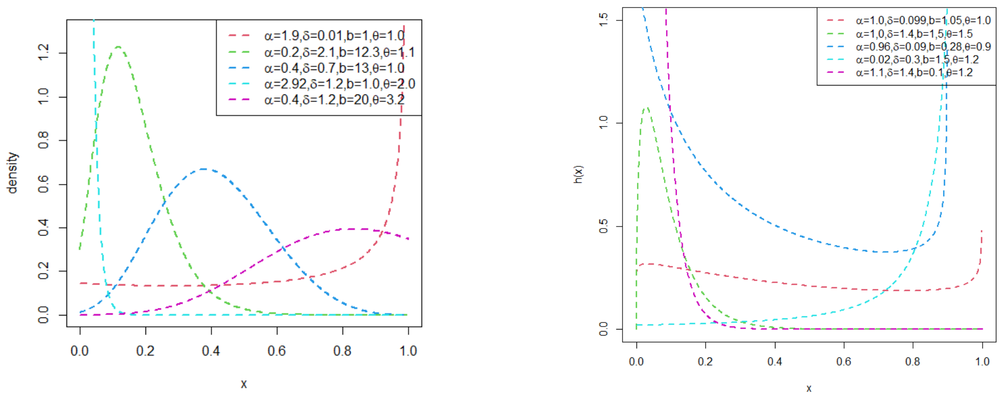

Figure 3: Some density and hrf plots for the TL-HT-TIIEHL-U distribution

Figure [3] shows that the TL-HT-TIIEHL-U distribution can be positively-skewed, negatively-skewed, almost symmetric, J and reversed-J shaped data. The hrf depicted in the plot exhibits both monotonic and non-monotonic patterns in its shape.

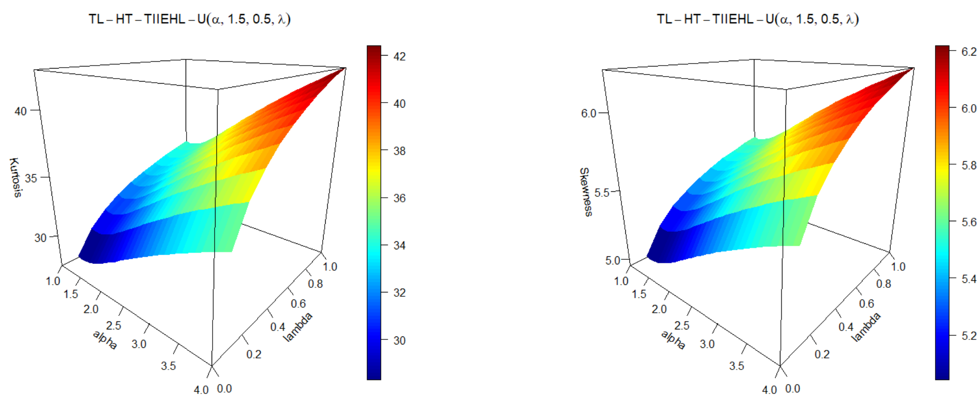

Figure 4: 3D Kurtosis and Skewness for the TL-HT-TIIEHL-U distribution

When the values of the parameters δ and θ are fixed, Figure [4] reveals that as δ and θ increase, the kurtosis and skewness of the TL-HT-TIIEHL-U distribution also increase.

2.9.3. Topp-Leone-Heavy-Tailed-Type II Exponentiated Half Logistic Weibull (TL-HT-TIIEHL-W) Distribution

The TL-HT-TIIEHL-W distribution is based on the Weibull distribution chosen as the baseline. Considering the one parameter Weibull distribution with cdf and pdf given by $G(x;\beta) = 1-\exp(-x^{\beta})$ and $g(x;\beta) = \beta x^{\beta-1}\exp(-x^{\beta})$, respectively, for $\beta, x > 0$ as the baseline distribution, we have the TL-HT-TIIEHL-W distribution with cdf

$$F(x;\alpha,\delta,b,\beta) = \left[1-\left(\frac{[A_3(x;\beta)]^{\delta}}{1-(1-\alpha)\left(1-[A_3(x;\beta)]^{\delta}\right)}\right)^{2\alpha}\right]^{b}$$

and pdf

$$
\begin{aligned}
f(x;\alpha,\delta,b,\beta) &= 4b\delta\alpha^2 \frac{\beta x^{\beta-1}[\exp(-x^\beta)]^\delta}{[2-\exp(-x^\beta)]^{\delta+1}} \left[1-\left(\frac{[A_3(x;\beta)]^\delta}{1-(1-\alpha)\left(1-[A_3(x;\beta)]^\delta\right)}\right)^{2\alpha}\right]^{b-1} \\
&\times \left(\frac{[A_3(x;\beta)]^{\delta(2\alpha-1)}}{\left[1-(1-\alpha)\left(1-[A_3(x;\beta)]^\delta\right)\right]^{2\alpha+1}}\right) \qquad (21)
\end{aligned}
$$

for $\alpha,\delta,b,\beta,x>0$, where $A_3(x;\beta)=\frac{\exp(-x^\beta)}{2-\exp(-x^\beta)}$. The hrf is

$$
\begin{aligned}
h(x;\alpha,\delta,b,\beta) &= 4b\delta\alpha^2 \frac{\beta x^{\beta-1}[\exp(-x^\beta)]^\delta}{[2-\exp(-x^\beta)]^{\delta+1}} \left[1-\left(\frac{[A_3(x;\beta)]^\delta}{1-(1-\alpha)\left(1-[A_3(x;\beta)]^\delta\right)}\right)^{2\alpha}\right]^{b-1} \\
&\times \left(\frac{[A_3(x;\beta)]^{\delta(2\alpha-1)}}{\left[1-(1-\alpha)\left(1-[A_3(x;\beta)]^\delta\right)\right]^{2\alpha+1}}\right)\left(1-\left[1-\left(\frac{[A_3(x;\beta)]^\delta}{1-(1-\alpha)\left(1-[A_3(x;\beta)]^\delta\right)}\right)^{2\alpha}\right]^b\right)^{-1}.
\end{aligned}
$$

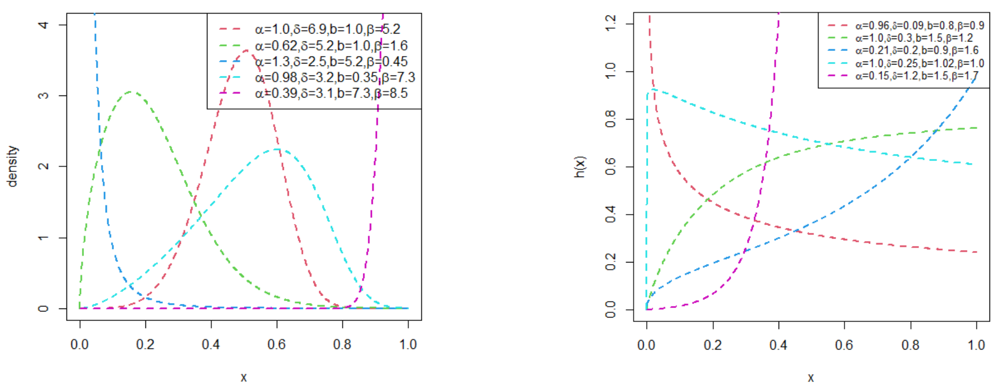

Figure 5: Density and hrf plots for the TL-HT-TIIEHL-W distribution

The graphical depictions presented in Figure [5] showcase the density and hrf plots associated with the TL-HT-TIIEHL-W distribution. The density of the TL-HT-TIIEHL-W can handle data that is positively skewed, negatively skewed, near symmetric, J and reversed-J shapes. The hrf is also capable of handling monotonic and non-monotonic geometries.

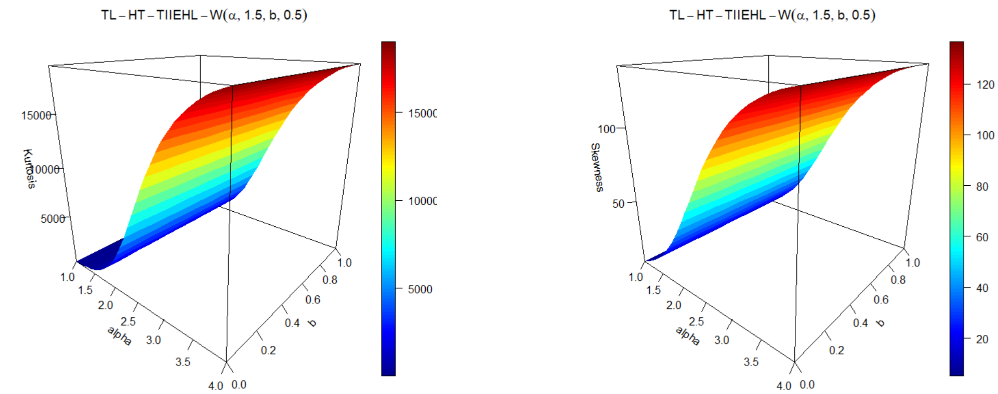

Figure 6: Visualization of 3D Kurtosis and Skewness for the TL-HT-TIIEHL-W distribution

When the parameters δ and β are held constant, Figure [6] illustrates that as α and b increase, the kurtosis and skewness of the TL-HT-TIIEHL-W distribution also increase.

3. Risk Measures

Risk measures are employed by actuaries to evaluate market risk. This section focuses on examining and analyzing various risk measures, including value at risk (VaR), tail value at risk (TVaR), tail variance (TV), and tail variance premium (TVP).

3.1. VaR

VaR provides an estimation of the potential downside risk associated with an investment or business activity. VaR_q, which is the q^{th} quantile for the TL-HT-TIIEHL-G FoDs is calculated from

$$VaR_q = G^{-1}\left(\frac{1+\left(\frac{(1-q^{\frac{1}{b}})^{\frac{1}{2\alpha}}-(1-\alpha)(1-q^{\frac{1}{b}})^{\frac{1}{2\alpha}}}{1-(1-\alpha)(1-q^{\frac{1}{b}})^{\frac{1}{2\alpha}}}\right)^{\delta}}{1-\left(\frac{(1-q^{\frac{1}{b}})^{\frac{1}{2\alpha}}-(1-\alpha)(1-q^{\frac{1}{b}})^{\frac{1}{2\alpha}}}{1-(1-\alpha)(1-q^{\frac{1}{b}})^{\frac{1}{2\alpha}}}\right)^{\delta}}\right), \tag{22}$$

for $\alpha, \delta, b > 0$ and $0 \leq q \leq 1$ is the probability level.

3.2. TVaR

TVaR is a risk metric that expresses the expected value of losses following the occurrence of an event that exceeds a predefined probability threshold. For the TL-HT-TIIEHL-G distribution, TVaR can be calculated as follows:

$$\begin{aligned} TVaR_q &= E\left(X|X > x_q\right) = \frac{1}{1-q}\int_{VaR_q}^{\infty} x f(x;\alpha,\delta,b,\varpi)dx \\ &= \frac{1}{1-q}\sum_{r=0}^{\infty}\int_{VaR_q}^{\infty} x\Phi_{r+1}g_{r+1}(x;\varpi)dx, \end{aligned} \tag{23}$$

where Φ_{r+1} is as given in Equation (14) and $g_{r+1}(x;\varpi) = (r+1)G^r(x;\varpi)g(x;\varpi)$ represents the exponentiated-G (Expo-G) pdf with power parameter $(r+1)$.

3.3. TV

TV is a measure that quantifies the conditional variance of losses in situations where they exceed the VaR with a given probability q. The TV_q of the TL-HT-TIIEHL-G distribution is given by

$$
\begin{aligned}
TV_q &= E\left(X^2 \mid X > x_q\right) - (TVaR_q)^2 \\
&= \frac{1}{1-q}\int_{VaR_q}^{\infty} x^2 f(x;\alpha,\delta,b,\varpi)dx - (TVaR_q)^2, \qquad (24)
\end{aligned}
$$

for $\alpha,\delta,b > 0$, ϖ represents the parameter vector from the baseline distribution and $0 \leq q \leq 1$.

3.4. TVP

Risk professionals often focus on risks that surpass specific thresholds, which is a common occurrence in insurance policies involving deductibles and reinsurance contracts. To address such scenarios, the TVP is utilized as a risk measure. The TVP of the TL-HT-TIIEHL-G distribution is expressed as

$$
TVP_q = TVaR_q + \phi(TV_q), \qquad (25)
$$

where $0 < \phi < 1$ is the sensitivity parameter that adjusts the contribution of TV to the TVP. Equations (23) and (24) are substituted into Equation (25) to find the TVP of the TL-HT-TIIEHL-G distribution.

3.5. Quantitative Analysis of the Risk Measures

The numerical simulations in this subsection provide results for various risk measures. These risk measures are evaluated for the TL-HT-TIIEHL-W distribution and compared to its nested models (with $\alpha = 1$, $\alpha = \beta = 1$), the odd power generalized Weibull-Weibull Poisson (OPGW-WP), type I heavy-tailed Weibull (TIHT-W) and the Weibull and distributions. The simulation results are obtained using the following methodology:

(1) stochastic samples of size 100 are generated from each distribution, and the parameters are estimated using MLE technique.

(2) a total of 1000 iterations are performed to calculate the risk measures for these distributions.

The results of the numerical analysis conducted on risk measures for a variety of nested and non-nested heavy-tailed distributions are displayed in Table [2]. Higher values of the risk metrics indicate distributions characterized by heavier tails. Among the analyzed distributions, the TL-HT-TIIEHL-W distribution shows a heavier tail. This suggests that the TL-HT-TIIEHL-W distribution is a suitable choice for modeling datasets that display heavy-tailed characteristics.

Table 2: Results of Risk Metrics Simulations

Significance level	Risk measure	0.60	0.65	0.70	0.75	0.80	0.85	0.90	0.95
TL-HT-TIIEHL-W($\alpha = 1.2, \delta = 0.35, b = 0.78, \beta = 1.1$)	VaR	2.0033	2.4442	2.9917	3.6907	4.6192	5.9289	7.9741	11.9430
	TVaR	6.7821	7.4275	8.2043	9.1652	10.4005	12.0834	14.6137	19.3134
	TV	33.8177	35.3126	36.9745	38.8382	40.9469	43.3443	46.0153	48.2969
	TVP	27.0727	30.3807	34.0864	38.2939	43.1580	48.9261	56.0275	65.1956
TL-HT-TIIEHL-W($\alpha = 1.0, \delta = 0.35, b = 0.78, \beta = 1.1$)	VaR	1.3851	1.6866	2.0592	2.5326	3.1576	4.0324	5.3851	7.9751
	TVaR	4.5578	4.9850	5.4975	6.1291	6.9373	8.0325	9.6678	12.6773
	TV	14.1941	14.7633	15.3907	16.0882	16.8717	17.7601	18.7678	19.8074
	TVP	13.0742	14.5812	16.2710	18.1953	20.4347	23.1285	26.5589	31.9443
TL-HT-TIIEHL-W($\alpha = 1.0, \delta = 0.35, b = 0.78, \beta = 1.0$)	VaR	0.2727	0.3669	0.4964	0.6800	0.9524	1.3859	2.1639	3.9743
	TVaR	2.1283	2.3865	2.7121	3.1363	3.7153	4.5623	5.9560	8.9033
	TV	11.2229	12.2517	13.4929	15.0227	16.9581	19.4835	22.8542	26.6332
	TVP	8.8620	10.3502	12.1571	14.4033	17.2818	21.1233	26.5247	34.2048
OPGWWP($\alpha = 1.2, \lambda = 0.5, \theta = 2.3, \beta = 1.1$)	VaR	0.0000	0.0001	0.0007	0.0025	0.0069	0.0178	0.0497	0.2566
	TVaR	0.0791	0.0905	0.1053	0.1256	0.1540	0.1949	0.2508	0.2000
	TV	0.0109	0.0115	0.0118	0.0118	0.0107	0.0077	0.0043	0.0532
	TVP	0.0857	0.0979	0.1136	0.1344	0.1625	0.2015	0.2547	0.2506
TIHT-W($\alpha = 1.2, \beta = 1.1$)	VaR	0.3172	0.5214	0.6712	0.9871	0.9722	1.3412	1.9745	3.0548
	TVaR	1.3246	1.4821	1.5614	2.0073	2.6701	2.9934	3.4218	4.3497
	TV	2.1647	2.7132	3.1933	4.4554	4.4316	4.6784	6.1237	7.164
	TVP	3.1023	4.2183	4.6187	5.2146	5.8724	6.8105	8.1647	8.4161
Weibull($\beta = 1.1$)	VaR	0.4806	0.5433	0.6147	0.6982	0.7989	0.9270	1.1046	1.4021
	TVaR	0.9270	0.9863	1.0544	1.1342	1.2310	1.3547	1.5270	1.8171
	TV	0.1891	0.1875	0.1857	0.1839	0.1818	0.1794	0.1765	0.1724
	TVP	1.0404	1.1082	1.1844	1.2721	1.3765	1.5072	1.6858	1.9809

4. Estimation

Within this specific section, we employ the maximum likelihood estimation (MLE) technique to derive parameter estimates for the TL-HT-TIIEHL-G distribution. We also consider estimation of the parameters of the new family of distributions for the censored case.

4.1. Maximum Likelihood Estimation

Suppose we have random variables X_i following a TL-HT-TIIEHL-G distribution, and let $\Lambda = (\alpha, \delta, b, \varpi)^T$ represent the model vector of parameters. In this context, the log-likelihood $\ell(\Lambda)$ for a sample of size n can be represented as

$$\begin{aligned}\ell(\Lambda) &= 2\ln(\alpha)+\ln(4b\delta)+\sum_{i=1}^{n}(\delta-1)\ln(1-G(x_i;\varpi))+\sum_{i=1}^{n}\ln(g(x_i;\varpi))+\sum_{i=1}^{n}(\delta+1)\ln(1-G(x_i;\varpi)) \\ &+ \sum_{i=1}^{n}(b-1)\ln\left[1-\left(\frac{\left[\frac{1-G(x;\varpi)}{1+G(x;\varpi)}\right]^{\delta}}{1-(1-\alpha)\left[1-\left[\frac{1-G(x;\varpi)}{1+G(x;\varpi)}\right]^{\delta}\right]}\right)^{2\alpha}\right]+\delta(2\alpha-1)\sum_{i=1}^{n}\ln\left[\frac{1-G(x;\varpi)}{1+G(x;\varpi)}\right] \\ &- \delta(2\alpha+1)\sum_{i=1}^{n}\ln\left[1-(1-\alpha)\left(1-\left[\frac{1-G(x;\varpi)}{1+G(x;\varpi)}\right]\right)\right]. \end{aligned} \tag{26}$$

The system of nonlinear equations $\left(\frac{\partial\ell}{\partial\alpha},\frac{\partial\ell}{\partial\delta},\frac{\partial\ell}{\partial b},\frac{\partial\ell}{\partial\varpi_k}\right)^T = \mathbf{0}$ can be solved numerically using the Newton-Raphson iteration method to estimate the parameters α, δ, b, and ϖ_k. The computation process can be facilitated by utilizing statistical software such as R, or other appropriate tools. The **web appendix** provides partial derivatives of the log-likelihood function with respect to each individual component of the score vector.

4.1.1. Estimation in the Presence of Censoring

Survival time studies often involve censored observations, where partial or interval censoring may occur, with right censoring being a specific type commonly observed in medical studies and predominantly represented by type I censoring in the field of survival analysis.

Consider a study comprising a random sample of n patients, with each patient having an independent censoring time denoted by $Y_i; i = 1,2,3,....,n$, that is, the time interval between entry and the end of the study, and $X_i; i = 1,2,...,n$, be the failure time of the i^{th} patient. The variables X_i and Y_i are assumed to be independent and follow the TL-HT-TIIEHL-G FoDs. For $T_i = min(X_i,Y_i),(T_i,u_i)$, u_i takes the value 0 if censoring occurs and 1 if failure is observed. Consequently, the log-likelihood function (ℓ) can be formulated in the following manner:

$$\ell = \sum_{i=1}^{n} u_i \log(f(t_i)) + \sum_{i=1}^{n}(1-u_i)\log(S(t_i)), \tag{27}$$

where $S(.) = 1-F(.)$ represents the survival function and $f(.)$ is the pdf of TL-HT-TIIEHL-G FoDs. The MLEs can be obtained by numerically maximizing the log-likelihood function specified in Equation (27).

5. Simulations

To evaluate the efficiency of the MLEs, a simulation study was carried out. The findings from the simulation are presented in Table 3. We simulated for n= 25, 80, 160, 250, 500 and 1000 for N=3000 from the TL-HT-TIIEHL-W distribution. The average bias (AvBIAS) and root mean square error (RMSEr) for an estimated parameter, say ($\hat{\delta}$), are computed using the following formulae:

$$AvBIAS(\hat{\delta}) = \frac{\sum_{j=1}^{N}\hat{\delta}_j}{N} - \delta, \quad \text{and} \quad RMSEr(\hat{\delta}) = \sqrt{\frac{\sum_{j=1}^{N}(\hat{\delta}_j-\delta)^2}{N}},$$

respectively. Based on the findings presented in Table 3, it is apparent that the mean values exhibit a high degree of proximity to the true parameter values as the sample size increases. Moreover, both the RTMSEr and the AvBIAS tend to approach zero across all parameters. This shows that the TL-HT-TIIEHL-W distribution produces efficient parameter estimates.

Table 3: Results of Monte Carlo Simulations for the TL-HT-TIIEHL-W Distribution: Mean, RMSEr, and AvBIAS

		$\alpha=0.9,\delta=0.01,b=0.25,\beta=2.5$			$\alpha=1.0,\delta=1.0,b=1.0,\beta=3.5$		
	n	Mean	RMSEr	AvBIAS	Mean	RMSEr	AvBIAS
α	25	1.0826	0.6208	0.1826	1.3470	0.9088	0.3470
	80	1.0027	0.3856	0.0927	1.2610	0.7149	0.2610
	160	1.0015	0.2849	0.0715	1.1110	0.3562	0.1110
	250	0.9903	0.2199	0.0597	1.0780	0.2723	0.0780
	500	0.9863	0.1350	0.0237	1.0411	0.1698	0.0411
	1000	0.9006	0.0849	0.0089	1.0178	0.1042	0.0178
δ	25	0.0407	0.0979	0.0307	1.3991	1.2173	0.5991
	80	0.0250	0.0922	0.0150	1.1858	0.9676	0.1858
	160	0.0162	0.0260	0.0062	1.1170	0.8690	0.1270
	250	0.0136	0.0136	0.0036	1.1103	0.8037	0.1103
	500	0.0122	0.0092	0.0022	1.0518	0.7001	0.0518
	1000	0.0111	0.0039	0.0011	1.0451	0.6411	0.0451
b	25	0.4473	1.5490	0.1973	1.9546	1.6987	1.9546
	80	0.2839	0.0924	0.0339	1.1925	0.8424	0.1925
	160	0.2709	0.0550	0.0209	1.0612	0.4123	0.0612
	250	0.2636	0.0384	0.0136	1.0471	0.3489	0.0471
	500	0.2576	0.0249	0.0076	1.0061	0.2315	0.0061
	1000	0.2502	0.0167	0.0049	1.0005	0.1783	0.0015
β	25	2.1988	0.8685	-0.3012	4.0870	2.7829	0.5870
	80	2.3309	0.5006	-0.1691	3.7237	1.1308	0.2237
	160	2.3766	0.3410	-0.1234	3.6326	0.7961	0.1326
	250	2.4209	0.2665	-0.0791	3.5693	0.6284	0.0693
	500	2.4459	0.1807	-0.0541	3.5645	0.5463	0.0645
	1000	2.4639	0.1246	-0.0361	3.5454	0.4783	0.0454

		$\alpha=1.0,\delta=3.5,b=0.2,\beta=3.5$			$\alpha=1.2,\delta=0.02,b=1.0,\beta=3.5$		
	n	Mean	RMSEr	AvBIAS	Mean	RMSEr	AvBIAS
α	25	1.3500	1.3316	0.3500	1.4870	1.4040	0.4870
	80	1.1106	0.4608	0.1106	1.2704	0.6941	0.2804
	160	1.0978	0.4155	0.0978	1.2719	0.5222	0.2719
	250	1.0810	0.4003	0.0810	1.2389	0.4066	0.2389
	500	1.0112	0.2505	0.0112	1.2373	0.3827	0.2373
	1000	1.0150	0.1801	0.0150	1.2010	0.0127	-0.1910
δ	25	3.9648	1.9495	1.3648	0.1043	0.7378	0.0843
	80	3.7253	1.7770	0.1253	0.0331	0.0532	0.0131
	160	3.5947	1.3580	0.0953	0.0283	0.0265	0.0083
	250	3.5401	1.2755	0.0699	0.0253	0.0174	0.0053
	500	3.5111	0.7669	0.0311	0.0235	0.0137	0.0035
	1000	3.5007	0.5487	0.0293	0.0218	0.0069	0.0018
b	25	0.4838	0.3970	0.7338	1.4167	0.6619	0.3067
	80	0.3042	0.1386	0.0542	1.2109	0.5984	0.2109
	160	0.2812	0.0847	0.0312	1.0843	0.2789	0.0843
	250	0.2743	0.0722	0.0243	1.0581	0.1996	0.0581
	500	0.2380	0.0467	0.0180	1.0315	0.1297	0.0315
	1000	0.2101	0.0295	0.0101	1.0153	0.0767	0.0153
β	25	3.8499	1.3139	0.3499	3.1724	0.8122	-0.3276
	80	3.7569	0.7833	0.2569	3.3468	0.4577	-0.1532
	160	3.6503	0.5788	0.1503	3.4090	0.3084	-0.0910
	250	3.6175	0.4816	0.1175	3.4275	0.2231	-0.0725
	500	3.5435	0.3754	0.0435	3.4510	0.1602	-0.0490
	1000	3.5110	0.0948	0.0090	3.4687	0.0969	-0.0313

6. Applications

The TL-HT-TIIEHL-W distribution is applied to real-world data and compared with various non-nested models, including established heavy-tailed distributions, in order to assess its performance. A comparison was made between the TL-HT-TIIEHL-W model and six other non-nested models namely, the odd exponentiated half logistic Burr XII (OEHLBXII) by Aldahlan and Afify (2018), the exponential Lindley odd log-logistic Weibull (ELOLLW) by Korkmaz et al. (2018), the Weibull Lomax (WL) by Tahir et al. (2014), the type II exponentiated half-logistic Topp-Leone-Weibull Poisson (TIIEHL-TL-WP) by Moakofiet al. (2021), the Burr III Topp-Leone-log-logistic (OBIII-TL-LLOG) by Chipepa et al. (2021) and the type I heavy-tailed-Weibull (TIHT-W) distributions by Zhao et al. (2020). See the **web appendix** for the pdfs of the distributions used in the comparisons.

The analysis incorporated a set of goodness-of-fit (GoF) statistics, encompassing the following measures: -2 log-likelihood ($-2\log(L)$), Akaike Information Criterion ($AIC = 2p - 2\log(L)$, Hannan-Quinn Information Criterion ($HQIC = -2\log(L) + 2p\ln[\ln(n)]$), Consistent Akaike Information Criterion ($CAIC = AIC + 2\frac{p(p+1)}{n-p-1}$), Bayesian Information Criterion ($BIC = p\log n - 2\log(L)$ (where n is the number of observed parameters, while the number of calculated parameters is p), Kolmogorov-Smirnov (K-S), Cramér-von Mises (W^*) and Andersen-Darling (AD). These statistics were used to verify the model that fits best for a given data set. The preferred model is determined by considering the one with the highest p-value for the K-S statistic and the lowest values for other statistical criteria. The sum of squares (SS) from the probability plots is used to calculate closeness to the diagonal line and is given as

$$SS = \sum_{i=1}^{n}\left[F_{TL-HT-TIIEHL-W}(x_{(i)};\hat{\alpha},\hat{\delta},\hat{b},\hat{\beta}) - \left(\frac{i-0.375}{n+0.25}\right)\right]^2, i = 1,2,3,....,n,$$

where $x_{(i)}$ is the i^{th} ordered observed data value. The TL-HT-TIIEHL-W model parameters were computed with the nonlinear minimization function (**nlm**) in R statistical software. Standard errors (SEs) (in parenthesis) accompany these parameter estimates for each data example. Probability plots with SS from the probability plots were also used to evaluate the fit. In addition, fitted densities, empirical cumulative distribution function (ECDF), Kaplan-Meier (K-M) survival curve, total time on test (TTT) plots and hazard rate function (hrf) plots are presented.

6.1. Growth Hormone Data

The initial data set includes the estimated duration, documented in 2009, from the administration of growth hormone medication to children until they reached the target age in the *Programa Hormonal de Secretaria de Saude de Minas Gerais*. This information was reported by Aldahlan and Afify (2018). The data set is contained in the **web appendix**.

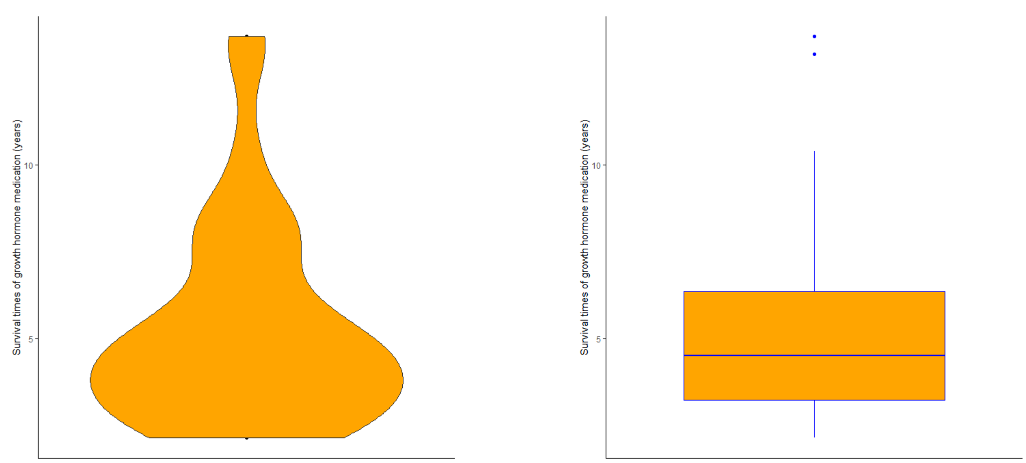

Figure 7: Violin and box plot for growth hormone medication

The descriptive statistics, visualized in the box plot and violin plot shown in Figure 7, indicate that the data exhibits positive skewness, meaning that the distribution is skewed towards higher values.

Table 4: Estimation and Statistical Analysis of Parameters for Growth Hormone Data

Distribution	Estimates and SEs				GoF Statistics								
					-2log(L)	AIC	CAIC	BIC	W^*	A^*	HQIC	K−S	p−value
	α	δ	b	β									
TL-HT-TIIEHL-W	0.0934	13.3720	301.7500	0.4567	155.2455	163.2455	164.5788	169.4668	0.0350	0.2532	165.3931	0.0865	0.9559
	(6.53×10^{-3})	(1.22×10^{-4})	(1.35×10^{-5})	(0.0558)									
	α	λ	a	b									
OEHLBXII	0.4337	0.0042	11.8416	0.2286	183.2828	191.2828	192.6162	197.5042	0.2654	1.6315	193.4305	0.1967	0.1333
	(0.1740)	(0.0088)	(0.0012)	(0.0687)									
	b	λ	θ	γ									
ELLOW	604.0800	3.4966	0.0312	1.3998	162.0604	170.0604	171.3938	176.2818	0.1253	0.7988	172.2080	0.1322	0.5732
	(2.12×10^{-4})	(9.4665)	(0.1183)	(0.1667)									
	a	b	α	β									
WL	66.4073	3.9403	0.1517	0.9619	161.4478	169.4478	170.7768	175.6648	0.1159	0.7433	171.5911	0.1284	0.6114
	(5.12×10^{-3})	(1.2092)	(0.0384)	(1.0907)									
	a	b	θ	λ									
TIIEHL-TL-WP	3.56×10^{-3}	2.2118	131.0700	0.1054	158.5477	166.5477	167.8826	172.7706	0.0569	0.3928	168.6969	0.6077	0.2954
	(8.27×10^{-4})	(0.7228)	(6.66×10^{-4})	(0.0180)									
	α	β	b	λ									
OBIII-TL-LLOG	1.1066	0.0954	1.0656	3.81×10^{-9}	173.6855	181.6855	183.0183	187.9064	0.2071	1.2918	183.8326	0.2333	0.0643
	(0.4732)	(0.0467)	(0.1572)	(0.0104)									
	α	θ	γ	–									
TIHT-W	2.2707	5.1903	3.56×10^{-4}	–	163.2748	169.2748	170.0490	173.9409	0.1409	0.8847	170.8855	0.1441	0.4617
	(0.2525)	(0.0167)	(3.58×10^{-4})	–									

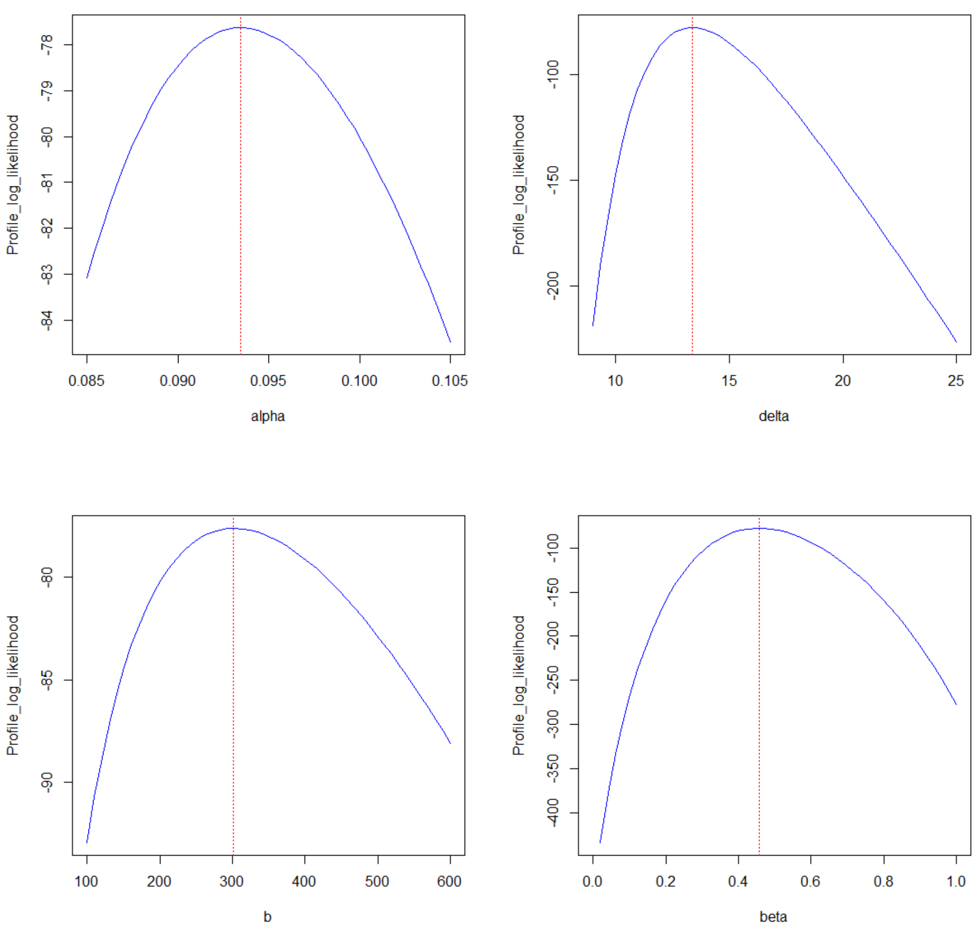

Figure 8: Profile log-likelihood plots illustrating TL-HT-TIIEHL-W parameters on growth hormone data

The TL-HT-TIIEHL-W parameters on growth hormone data can be uniquely identified, as shown in Figure [8]. The GoF statistics and MLEs for the models are shown in Table [4]. The estimated variance-covariance (vcov) matrix is

 DOI: https://doi.org/10.18187/pjsor.v21i2.4640

$$\begin{bmatrix} 4.27\times10^{-5} & 7.66\times10^{-7} & -8.01\times10^{-8} & -3.29\times10^{-4} \\ 7.66\times10^{-7} & 1.48\times10^{-8} & -1.62\times10^{-9} & -6.68\times10^{-6} \\ -8.01\times10^{-8} & -1.62\times10^{-9} & 1.81\times10^{-10} & 7.50\times10^{-7} \\ -3.29\times10^{-4} & -6.68\times10^{-6} & 7.50\times10^{-7} & 3.11\times10^{-3} \end{bmatrix}.$$

The model parameters' asymptotic confidence intervals at a 95% confidence level are as follows: $\alpha \in [0.0935 \pm 0.0128]$, $\delta \in [13.3720 \pm 1.17\times10^{-4}]$, $b \in [301.7500 \pm 2.64\times10^{-5}]$ and $\beta \in [0.4567 \pm 0.1093]$, respectively.

The TL-HT-TIIEHL-W mode1 is superior to the several non-nested models that were taken into consideration, according to the GoF statistics and K-S p-values obtained on growth hormone data.

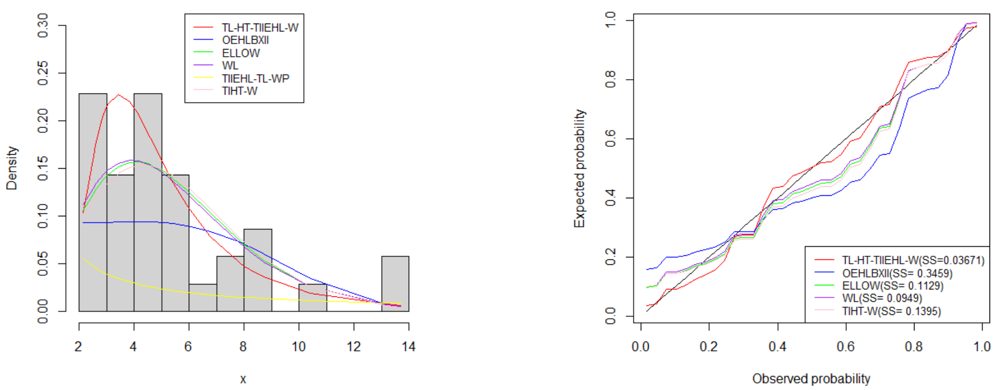

Figure 9: Graphical representations of the fitted density functions and probability plots for the growth hormone data

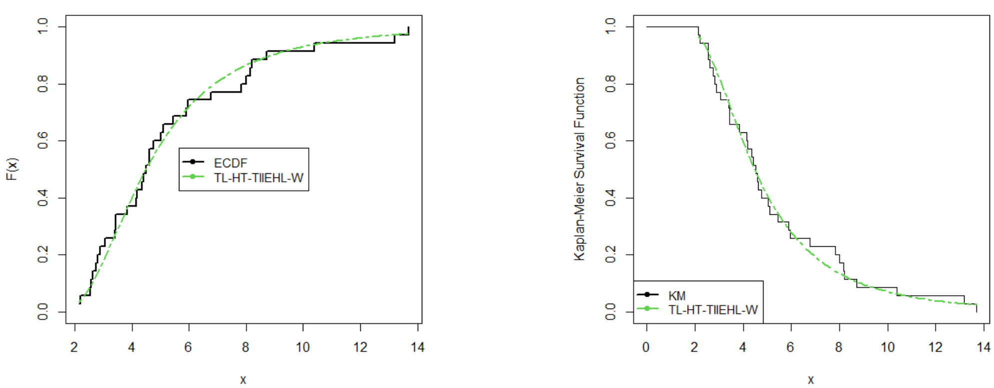

Figure 10: Fitted ECDF curve and K-M plots for growth hormone data

The plots illustrated in Figure [9] indicate that the TL-HT-TIIEHL-W distribution demonstrates superior performance compared to the non-nested models when applied to the growth hormone data. The graphical representation depicted in Figure [10] illustrates the observed and fitted ECDF as well as the K-M survival curves for the growth hormone data. The plots demonstrate that the TL-HT-TIIEHL-W distribution closely aligns with the observed ECDF and K-M survival curves.

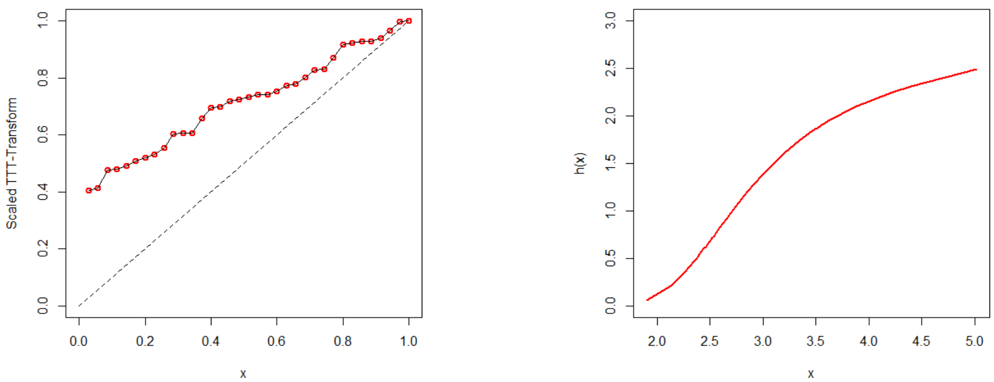

Figure 11: Fitted TTT scaled and hrf plots for growth hormone data

Figure [11] exhibits the TTT scaled plot and hrf plots, which reveal an increasing hazard rate pattern for the growth hormone data.

6.2. Head and Neck Data: Complete Case

The second set of data comprises survival times, measured in days, for a group of forty (40) patients who have been diagnosed with head and neck cancer. The data was subjected to analysis using the methodology proposed by Efron (1988) and was later analyzed by Salerno, S. and Li (2023). The data is presented in the **web appendix**.

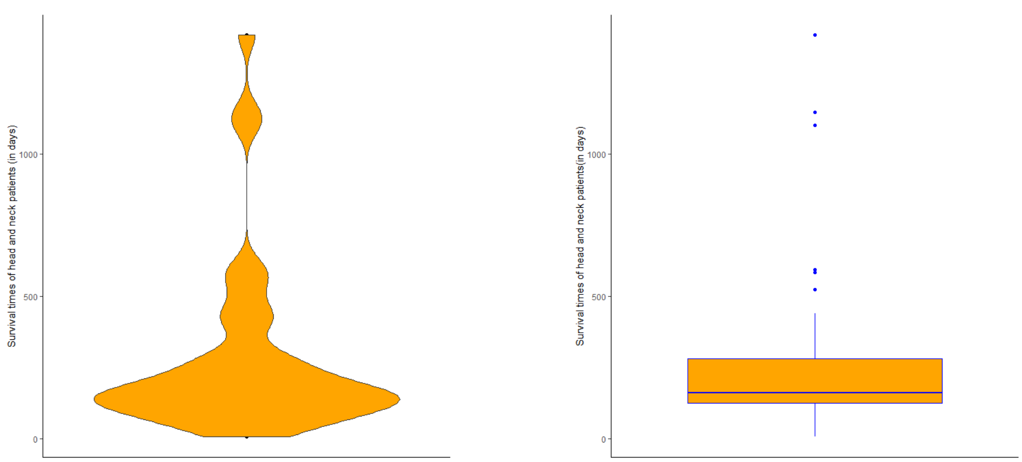

Figure 12: Violin and box plot for head and neck data

The displayed violin plot and box plot for the survival times of head and neck cancer patients in Figure [12] suggest positive skewness.

Table 5: Estimation and Statistical Analysis of Parameters for Head and Neck Cancer Data

					GoF Statistics								
Distribution	Estimates and SEs				-2log(L)	AIC	CAIC	BIC	W^*	A^*	HQIC	K−S	p−value
	α	δ	b	β									
TL-HT-TIIEHL-W	3.1606	0.0033	4.4469	0.6619	525.5643	533.5643	534.7072	540.3198	0.1132	0.6212	536.0069	0.1252	0.5578
	(4.58×10^{-4})	(1.27×10^{-3})	(3.48×10^{-3})	(7.10×10^{-2})									
	α	λ	a	b									
OEHLBXII	0.3910	5.15×10^{-5}	2.5547	0.6244	552.6971	560.6971	561.8399	567.4226	0.3963	2.2409	563.1397	0.2192	0.0428
	(0.0404)	(3.28×10^{-5})	(8.84×10^{-3})	(0.0362)									
	b	λ	θ	γ									
ELLOW	408.9700	1.2249	0.0269	0.7517	527.9122	535.9122	537.0551	542.6677	0.1749	0.9603	538.3548	0.1489	0.3375
	(5.22×10^{-4})	(10.8040)	(0.1785)	(0.0847)									
	a	b	α	β									
WL	100.9200	1.9149	0.0648	92.9160	526.7091	534.7091	534.8520	540.4646	0.1215	0.6628	536.1517	0.1261	0.4482
	(7.22×10^{-5})	(0.2105)	(0.0154)	(1.04×10^{-3})									
	a	b	θ	λ									
TIIEHL-TL-WP	11.1000	2.47×10^{-2}	0.2005	5.13×10^{-9}	592.4668	600.4468	601.6106	607.2233	0.1389	0.7727	602.9103	0.4854	0.0923
	(9.1429)	(2.03×10^{-2})	(4.80×10^{-2})	(8.66×10^{-3})									
	α	β	b	λ									
OBIII-TL-LLOG	8.7349	50.0587	0.8885	0.0808	534.2370	542.2370	543.3798	548.9925	0.1724	1.0493	544.6796	0.1569	0.2784
	(5.01×10^{-5})	(4.16×10^{-3})	(0.2655)	(5.43×10^{-3})									
	α	θ	γ	–									
TIHT-W	1.2407	2.9439	1.22×10^{-4}	–	528.1106	534.1106	534.7773	540.7772	0.1810	0.9894	536.9425	0.1466	0.3566
	(0.1434)	(2.62×10^{-4})	(1.05×10^{-4})	–									

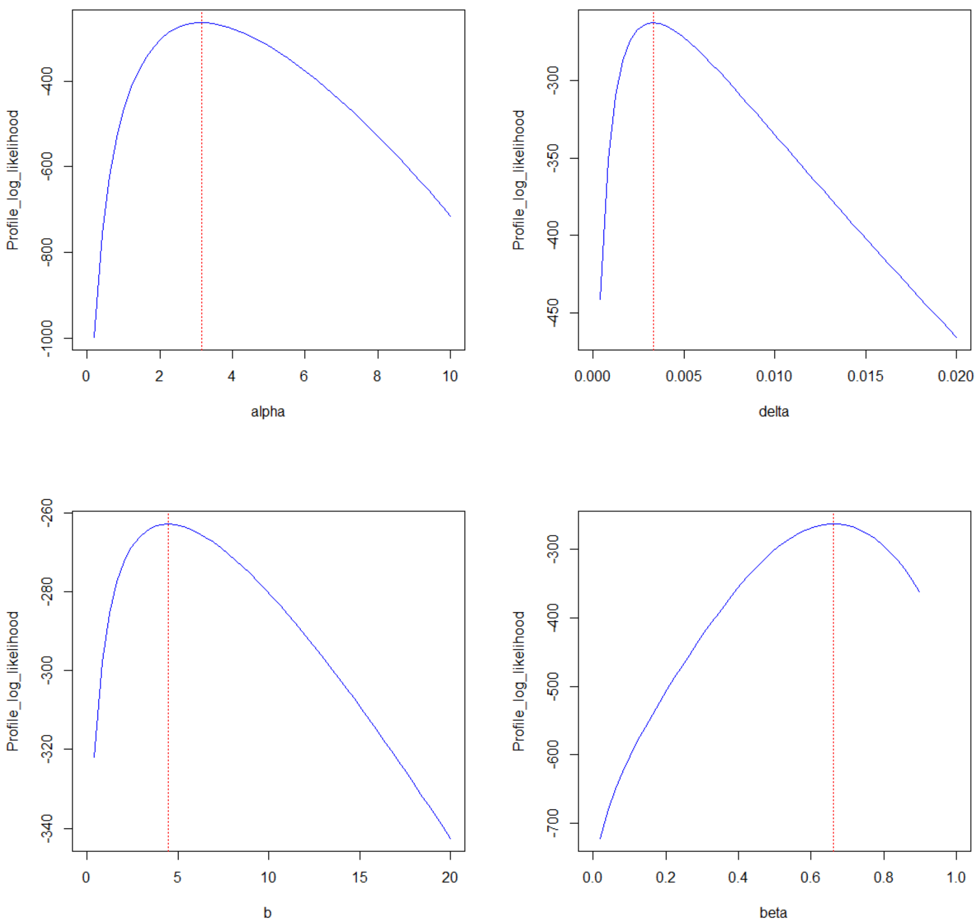

Figure 13: Profile log-likelihood plots illustrating TL-HT-TIIEHL-W parameters on head and neck cancer data

The TL-HT-TIIEHL-W parameters on head and neck cancer data can be uniquely identified, as shown in Figure [13]. The GoF statistics and MLEs for the models are shown in Table [5]. The estimated vcov matrix is

$$\begin{bmatrix} 2.10\times10^{-7} & -5.63\times10^{-7} & 1.59\times10^{-6} & 3.26\times10^{-5} \\ -5.63\times10^{-7} & 1.61\times10^{-6} & -4.27\times10^{-6} & -8.73\times10^{-5} \\ 1.59\times10^{-6} & -4.27\times10^{-6} & 1.21\times10^{-5} & 2.47\times10^{-4} \\ 3.26\times10^{-4} & -8.73\times10^{-5} & 2.47\times10^{-4} & 5.05\times10^{-3} \end{bmatrix}.$$

The model parameters' asymptotic confidence intervals at a 95% confidence level are as follows: $\alpha \in [3.1606 \pm 8.98\times10^{-4}]$, $\delta \in [0.0033 \pm 2.49\times10^{-3}]$, $b \in [4.4469 \pm 6.82\times10^{-3}]$ and $\beta \in [0.6619 \pm 0.1392]$, respectively.

The TL-HT-TIIEHL-W mode1 is superior to the several non-nested models that were taken into consideration, according to the GoF statistics and K-S p-values obtained on head and neck cancer data.

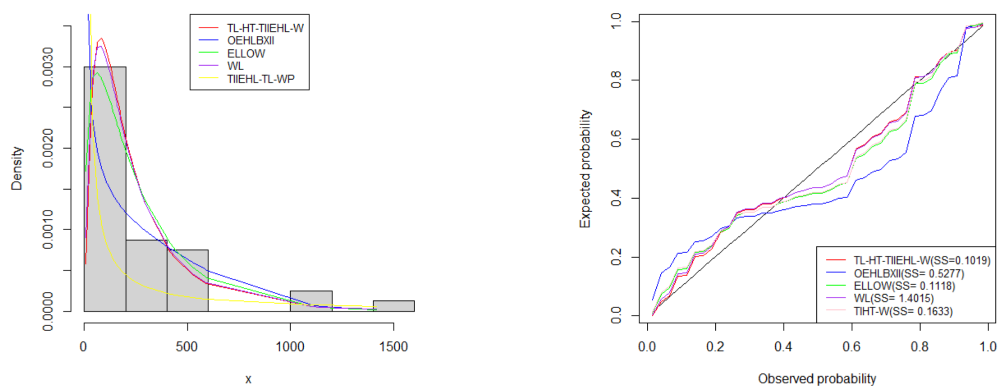

Figure 14: Graphical representations of the fitted density functions and probability plots for the head and neck cancer data

The results illustrated in Figure [14] indicate that the TL-HT-TIIEHL-W distribution demonstrates superior performance compared to the non-nested models when applied to the head and neck cancer data.

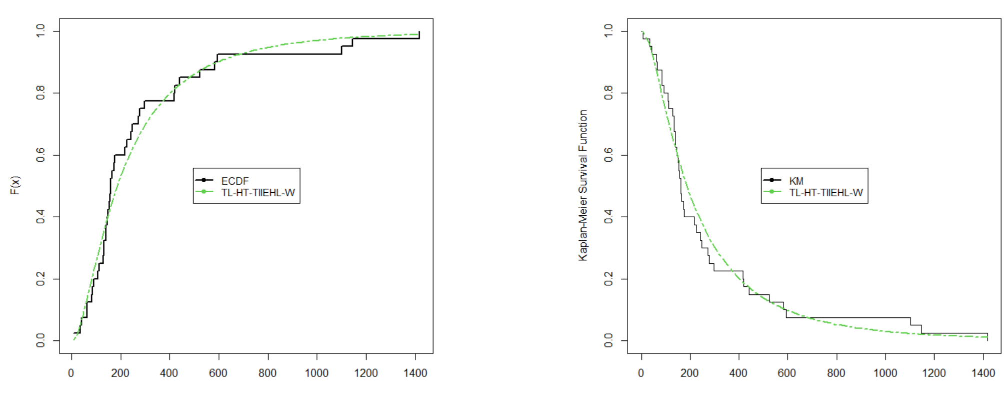

Figure 15: Fitted ECDF curve and K-M plots for head and neck data

The graphical representation presented in Figure [15] displays both the observed and fitted ECDF as well as the K-M survival curves for the head and neck cancer data. The plots indicate that the TL-HT-TIIEHL-W distribution closely adheres to the observed ECDF and K-M survival curves.

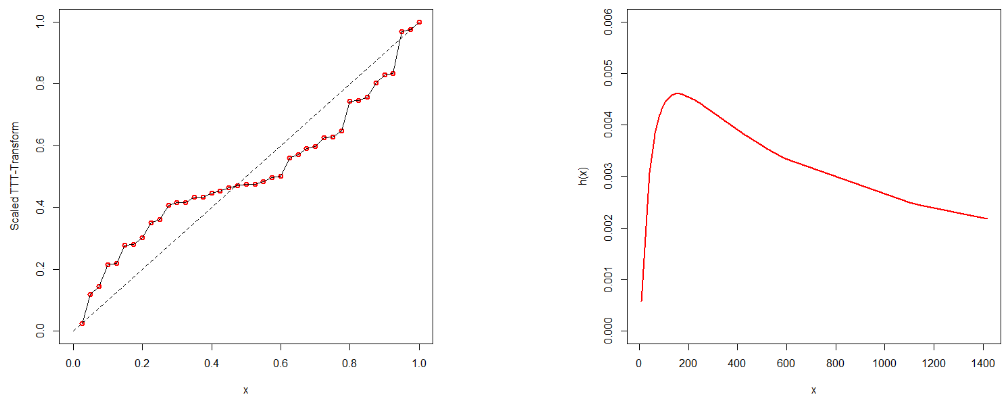

Figure 16: Fitted TTT scaled and hrf plots for head and neck cancer data

The TTT scaled plot and hrf plots in Figure [16] depict an inverted bathtub hazard rate shape for head and neck cancer data.

6.2.1. Head and Neck Data: Censored Case

The second set of data gives the survival times (in days) of forty-nine (49) patients diagnosed with head and neck cancer disease. The data includes nine (9) censored observations. The data is presented in the **appendix**.

Table 6: Parameter Estimates and Statistics for Head and Neck Data: Censored Case

					GoF Statistics				
Distribution	Estimates and SEs				-2log(L)	AIC	CAIC	BIC	SS
	α	δ	b	β					
TL-HT-TIIEHL-W	17.4230	8.91×10^{-4}	21.4180	0.3243	559.4459	567.4459	568.3550	566.2067	0.1032
	(2.32×10^{-5})	(1.45×10^{-4})	(1.21×10^{-4})	(0.0330)					
	α	λ	a	b					
OEHLBXII	0.5647	1.20×10^{-3}	1.2497	0.8457	587.8382	595.8382	596.7473	594.5990	0.3756
	(0.1172)	(9.86×10^{-4})	(0.2374)	(0.1621)					
	b	λ	θ	γ					
ELLOW	293.9700	6.8300	0.0151	0.6235	563.7935	571.7935	572.7026	570.5543	0.1217
	(5.22×10^{-4})	(10.8040)	(0.1785)	(0.0847)					
	a	b	α	β					
WL	54.3940	1.7231	0.0545	82.8050	559.4890	567.4890	568.3981	566.2498	0.1204
	(1.31×10^{-4})	(0.1995)	(0.0140)	(1.03×10^{-3})					
	a	b	θ	λ					
TIIEHL-TL-WP	2.44×10^{-3}	2.4577	131.0600	0.0670	640.3144	648.3144	649.2235	647.0752	0.1652
	(5.59×10^{-4})	(0.8170)	(1.04×10^{-3})	(0.0113)					
	α	β	b	λ					
OBIII-TL-LLOG	10.3660	27.7990	1.1994	0.0569	561.3835	569.3835	570.2926	568.1443	2.3156
	(2.28×10^{-5})	(0.0144)	(0.3457)	(4.16×10^{-3})					
	α	θ	γ	–					
TIHT-W	1.0230	2.6973	3.28×10^{-4}	–	564.5581	572.5581	573.0914	569.6287	0.1392
	(0.1236)	(4.22×10^{-4})	(2.52×10^{-4})	–					

Table [6] displays the MLEs of the unknown parameters for the TL-HT-TIIEHL-W distribution, which were obtained using censored data. These estimates were obtained by maximizing the log-likelihood function, specified in Equation (27), which serves as the objective function for the estimation process. The corresponding SEs of MLEs are presented within the parentheses. The estimated vcov matrix is

$$\begin{bmatrix} 5.40\times10^{-10} & -3.19\times10^{-9} & 2.80\times10^{-9} & 7.66\times10^{-7} \\ -3.19\times10^{-9} & 2.09\times10^{-8} & -1.67\times10^{-8} & -4.54\times10^{-6} \\ 2.80\times10^{-9} & -1.67\times10^{-8} & 1.46\times10^{-8} & 3.98\times10^{-6} \\ 7.66\times10^{-7} & -4.54\times10^{-6} & 3.98\times10^{-6} & 1.09\times10^{-3} \end{bmatrix},$$

and the asymptotic confidence intervals at 95% confidence level for the model parameters are: $\alpha\in[17.4230\pm4.55\times10^{-5}]$, $\delta\in[8.91\times10^{-4}\pm2.83\times10^{-3}]$, $b\in[21.4180\pm2.37\times10^{-4}]$ and $\beta\in[0.3243\pm0.0647]$, respectively. The TL-HT-TIIEHL-W model out-performs the non-nested models that were considered according to the GoF obtained on head and neck cancer censored data.

7. Conclusions and Recommendations

In conclusion, this study introduced the Topp-Leone-heavy-tailed type II exponentiated half-logistic-G (TL-HT-TIIEHL-G) FoDs, providing a valuable tool for modeling heavy-tailed data. The statistical properties of the TL-HT-TIIEHL-G FoDs were examined, and actuarial risk measures were derived and analyzed. The study demonstrated the superiority of the TL-HT-TIIEHL-G FoDs over some existing non-nested models by fitting the TL-HT-TIIEHL-W distribution (a particular case of the TL-HT-TIIEHL-G) to three real-life data sets. The TL-HT-TIIEHL-G FoDs demonstrated its capacity to accommodate both monotonic and non-monotonic hazard rate patterns. The findings highlighted the practical applicability of the TL-HT-TIIEHL-G FoDs in various domains including health and reliability analysis, where accurate modeling of heavy-tailed phenomena is crucial for risk assessment and decision-making.

Although this study offers notable advancements in the realm of distribution theory, it is crucial to recognize and acknowledge its inherent limitations. The empirical evaluation of the TL-HT-TIIEHL-G FoDs is based on specific data sets, limiting the generalizability of the findings to other domains and data sets. Furthermore, the study solely relies on maximum likelihood estimation for parameter estimation, leaving room for exploring alternative methods, such as Bayesian estimation. Future research directions include incorporating Bayesian estimation techniques and exploring computational efficiency for large data sets. These endeavors will further enhance our understanding and utilization of the TL-HT-TIIEHL-G family in statistical modeling and analysis.

To access the appendix, kindly click on the link provided below:
https://drive.google.com/file/d/1yVKs-AyF2SLGwwWF9-jgZQiZwYxxn-3D/view?usp=sharing

References

Al-Mofleh, H., Elgarhy, M., Afify, A. Z., & Zannon, M. S. (2020). Type II exponentiated half logistic generated family of distributions with applications. Electronic Journal of Applied Statistical Analysis, 13(2), 536–561.

Al-Shomrani, A., Arif, O., Shawky, A., Hanif, S., & Shahbaz, M. Q. (2016). Topp-Leone family of distributions: Some properties and applications. Pakistan Journal of Statistics and Operation Research, 12(3), 443–451.

Alizadeh, M., Bagheri, S., Bahrami, S. E., Ghobadi, S., & Nadarajah, S. (2018). Exponentiated power Lindley power series class of distributions: Theory and applications. Communication Statistics Simulation Computing, 47(2), 2499–2531.

Aldahlan, M., & Afify, A. Z. (2018). The odd exponentiated half-logistic Burr XII distribution. Pakistan Journal of Statistics and Operation Research, 14(2), 305-317.

Chesneau, C., Sharma, V. K., & Bakouch, H. S. (2021). Extended Topp-Leone family of distributions as an alternative to Beta and Kumaraswamy type distributions: Application to glycosaminoglycans concentration level in urine. International Journal of Biomathematics, 14(2), 2050088.

Chipepa, F., and Oluyede, B. (2021). The Topp-Leone odd exponential half logistic-G family of distributions: Model, properties and applications. Pakistan Journal of Statististics, 37(3):253–277.

Chipepa, F., Oluyede, B. O., & Peter, O. P. (2021). The Burr III Topp-Leone-G family of distributions with applications. Heliyon, 7(4), 1–16.

Efron B. (1988). Logistic regression, survival analysis, and the Kaplan-Meier Curve. Journal of the American statistical Association, 83(4), 414–425.

Hamedani, G., Korkmaz, M., Butt, N. & Yousof, H. (2020). The type II quasi Lambert-G family of probability distributions. Pakistan Journal of Statistics and Operations Research, (18), 963–983.

Jamal, F., Chesneau, C., & Elgarhy, M. (2020). Type II general inverse exponential family of distributions. Journal of Statistics and Management Systems, 23(3), 617-641.

Korkmaz, M. C., Yousof, H. M., & Hamedani, G. G. (2018). The exponential Lindley odd log-logistic-G family: Properties, characterizations and applications. Journal of Statistical Theory and Applications, 17(3), 554-571.

Marganpoor, S., Ranjbar, V., Alizadeh, M., & Abdollahnezhad, K. (2020). Generalised odd Fréchet family of distributions: Properties and applications. Statistics in Transition new series, 21(3), 109-128.

Moakofi, T., Oluyede, B., & Chipepa, F. (2021). Type II exponentiated half-logistic-Topp-Leone-G power series class of distributions with applications. Pakistan Journal of Statistics and Operation Research, 17(4), 885-909.

Oluyede, B., Chamunorwa, S., Chipepa, F., & Alizadeh, M. (2022). The Topp-Leone Gompertz-G family of distributions with applications. Journal of Statistics and Management Systems, 25(8), 1-25

Oluyede, B., Dingalo, N., & Chipepa, F. (2023). The Topp-Leone-Harris-G family of distributions with applications. International Journal Mathematics in Operational Research, 24(4), 554-582.

Oluyede, B., & Moakofi, T. (2023). The Gamma-Topp-Leone-type II-exponentiated half logistic-G family of distributions with applications. Stats, 6, 706–733.

Rényi, A. (1960). On measures of entropy and information. Proceedings of the fourth Berkeley symposium on mathematical statistics and probability. University of Carlifonia Press, Berkeley and Los Angeles, 1, 547-561.

Salerno, S., & Li, Y. (2023). High-dimensional survival analysis: Methods and applications. Annual Review of Statistics and its Application, 10(1), 25-49.

Shaked, M., & Shanthikumar, J. G. (2007). Stochastic orders. Springer, New York.

Shah, Z., Khan, D. M., Khan, Z., Faiz, N., Hussain, S., Anwar, A., Ahmad, T., & Kim, K. I. (2023). A new generalized logarithmic–X family of distributions with biomedical data analysis. Applied Sciences, 13(6), 3668.

Shannon, C. E. (1950). Prediction and entropy of printed English. The Bell System Technical Journal, 30, 50-64.

Tahir, M., Cordeiro, G. M., & Zubair, M. (2014). The Weibull-Lomax distribution: Properties and applications. Hacettepe University Bulletin of Natural Sciences and Engineering Series B: Mathematics and Statistics, 44, 1-24.

Zhao, W., Khosa, S. K., Ahmad, Z., Aslam M., & Afify, A. Z. (2020). Type-I heavy-tailed family with applications in medicine, engineering and insurance. PLoS ONE, 15(8), 63-79.